U.S. - JAPAN COOPERATIVE RESEARCH ON R/C FULL-SCALE BUILDING TEST
Part 5 DISCUSSION ON DYNAMIC RESPONSE SYSTEM

T. Kabeyasawa (I)
H. Shiohara (II)
S. Otani (III)
Presenting Author: T. Kabeyasawa

SUMMARY

Pseudo-dynamic earthquake response tests of the full-scale seven-story reinforced concrete structure were simulated by a nonlinear dynamic analysis method. Calculated response waveforms, hysteresis relations and local deformations were compared with the test results. A good correlation was reported between the observed and calculated responses. Nonlinear earthquake response analysis was carried out to study the effect of higher modes on the shear force in the wall during an earthquake.

INTRODUCTION

This paper describes a computer analysis of the full-scale seven-story reinforced concrete test structure. A general purpose computer program was developed to simulate the inelastic earthquake response of a structure including shear walls. On the basis of given structural geometry and material properties, this paper places an emphasis to clarify (a) method to model member behavior, and (b) method to determine member stiffness properties. The information from the results of the full-scale test and the small-scale subassemblage tests was reflected in the development of analytical methods. The analytical method is useful to understand the overall structural behavior and the local behavior.

The full-scale structure was tested using "equivalent" single-degree-of-freedom pseudo-dynamic response (SPD) test procedure. However, the maximum wall shear force in a multi-degree-of-freedom dynamic response may be higher than that observed in SPD tests, due to the effect of higher modes. From a viewpoint of the ultimate-state design of ductile shear walls, it is important to evaluate the possible maximum shear force input to a wall during an earthquake. This paper also reports on the dynamic magnification of the wall shear force computed from nonlinear earthquake response analysis of the wall-frame structure.

STRUCTURAL IDEALIZATION

A general plan view and an elevation of the full-scale test structure are shown in Figure 1 <Ref. 1>. The structure was idealized as plane frames. Floor slab was assumed to be rigid in its own plane, causing identical horizontal displacement of all the joints in a floor level. The mass of the structure was assumed to be concentrated at each floor level. Vertical

---

(I) Research Associate, Yokohama National University, Japan
(II) Graduate Student, University of Tokyo, Japan
(III) Associate Professor, University of Tokyo, Japan

displacement and rotation were the two degrees of freedom at each joint. The frames and a shear wall were assumed to be fixed at the base of the structure. Three different member models were used in the analysis.

Beam and Column Model : The one-component model was used for beams and columns. Axial deformation was considered in a column member. A beam-to-column connection panel was assumed to be rigid.

Wall Model : The full-scale tests and support tests of half-scale shear wall subassemblies <Ref. 2> indicated that the bending deformation of a wall was accompanied by the significant extension of the outside columns. The wall was, therefore, idealized as three vertical line elements with infinitely rigid beams at the top and bottom floor levels (Fig. 2). Two outside truss elements represented the axial stiffness of the boundary columns. The axial stiffness varied with the sign and level of axial stress. The central element was a one-component model with vertical, horizontal and rotational springs.

Transverse Beam Model : The transverse beam connecting the outside column of a shear wall and an adjacent parallel open frame is subjected to differential vertical displacement, and, in turn, increases the vertical load on the tensile boundary column. Vertical spring elements were introduced to reflect the effect of such transverse beams (Fig. 3).

HYSTERESIS MODELS

Two different hysteresis models were developed and used for nonlinear springs of member models.

Takeda-Slip Hysteresis Model : Half-scale beam-to-column joint assemblies were tested <Ref. 3> to obtain preliminary information about possible behavior of the full-scale structure. Force-deformation relation of a beam with slab showed obvious pinching characteristics in a negative moment region. Takeda-Slip Hysteresis model (Fig. 4) was developed introducing pinching characteristics into Takeda Hysteresis model <Ref. 4> with simplified rules for inner loops, and was used in the nonlinear beam and transverse beam models. The pinching was assumed to occur only in negative moment in case of the beam model. Simplified Takeda Hysteresis model without rules for pinching was used in the rotational springs of the column and wall model.

Axial-Stiffness Hysteresis Model : The behavior of reinforced concrete member under axial load reversals is not clearly understood. Referring to the moment-axial deformation relations observed in half-scale shear wall assembly tests <Ref. 2>, Axial-Stiffness Hysteresis model (Fig. 5) was developed and used for the axial force-deformation relation of the three vertical line elements of the wall model.

STIFFNESS OF MEMBER MODELS

Force-deformation relationship under monotonically increasing load was evaluated on the basis of idealized stress-strain relation of the concrete and the reinforcing steel.

Beam Stiffness : The beams were analyzed as a T-shaped beam. The effective slab width of 150 cm for the elastic stiffness was taken in accordance

with the AIJ Standard <Ref. 5>. Cracking moment was computed on the basis of the flexural theory and an assumed concrete tensile strength. Yield moment and curvature were calculated based on the flexural theory and the idealized stress-strain relationships for steel and concrete. The slab effective width of 430 cm was used in computation of yield moment and curvature because the strains measured in the slab reinforcing bars during the full-scale test indicated that the effective width of slab was from 350 cm to 510 cm at the maximum structural deformation. The beam-end rotations were computed on the basis of corresponding curvature distribution of the beam with an inflection point at the mid-span. The stiffness after yielding was assumed to be 3 % of the initial elastic stiffness.

Column Stiffness : Simple approximate expressions from the AIJ Standard <Ref. 5> were used to evaluate cracking and yielding moment of a column section. The yield rotations were evaluated by a simple empirical formula by Sugano <Ref. 6>.

Wall Stiffness : The axial rigidity of three vertical line elements was assumed to remain linearly elastic in compression. When a net axial load changed its sign from compression to tension, the stiffness was reduced to 90 % of the initial elastic stiffness. Tensile yielding occurred when a net tensile force reached a force level at which all longitudinal reinforcement yielded. Then the stiffness was reduced to 0.1 % of the initial elastic stiffness. Cracking of the rotational spring of the central vertical element was to occur when the extreme tensile fiber strain became zero under the gravity load and overturning moment. Yield moment was taken to be the full plastic moment of all vertical wall reinforcement. The stiffness after yielding was taken to be 0.1 % of the initial elastic stiffness. The shear rigidity was defined by the wall sectional area and shape factor, and was assumed to remain elastic.

ANALYSIS OF PSEUDO-DYNAMIC TESTS

The analytical method described above was applied to the full-scale test structure. The test was carried out using " SPD test procedure <Ref. 1>." The structure was subjected to lateral load of an inverted triangular distribution. The response under an imaginary earthquake motion was computed for a reduced SDF system having the observed restoring force characteristics of the test structure, to control the roof-level displacement. No damping was assumed in the pseudo-dynamic response computation during the test. A numerical procedure was developed to simulate the SPD test procedure.

The intensity of input earthquake motions was varied in four test runs (SPD-1 to SPD-4) to yield expected maximum roof-level displacements of approximately 1/7000, 1/400, 3/400, and 1/75 of the total height. The higher frequency components of the input base acceleration were removed from the original record so that the first mode should govern the response of the test structure. The second through fourth pseudo-dynamic tests were simulated continuously. The analytical results such as response waveforms, hysteresis relations and local deformations were compared with the test results.

Response Waveforms : Observed and calculated response waveforms are compared for the roof-level displacement and base shear (Fig. 6). At the end of each test run, pseudo-dynamic free-vibration test was started with existing

residual displacement and no velocity. Analytical response (solid lines) are in good agreement with the observed (broken lines) except for the latter part of SPD-2. Post-yielding stiffness of constituent members of an analytical model described above was determined, so that calculated maximum base shear amplitude in the test SPD-3 would agree with the observed.

Hysteresis relations : Pseudo-dynamic response computation was carried out using observed hysteresis relations between the roof-level displacement and the base shear (SDF hysteresis). The observed and computed SDF hysteresis relations (Fig.7) are in fair agreement, especially at the peaks of hysteresis shapes. However, the calculated stiffness and resistance (solid lines) were generally lower than the observed (broken lines) in the test SPD-2. The calculated stiffness in a small oscilation following a large amplitude was lower, which might cause the discrepancy in the response waveforms in the latter part of SPD-2. The analytical model showed some pinching behavior in SPD-3 and 4, which was also noted in the observed hysteresis relations.

Beam End Rotations : Computed local deformations of typical members were compared with those observed during the test SPD-3. Flexural rotations at beam ends were measured by two displacement gauges. The gauge length was one half the effective beam depth (22 cm) from the column face. The observed and computed base shear-beam end rotation relations of a sixth floor beam at the wall connection are shown in Fig. 8 (a) and (b). General hysteresis shapes were similar. However, the observed beam end rotations were proportionally smaller, approximately 60 to 70 % of the calculated amplitudes because the rotation was measured for a given gauge length, whereas the rotation was calculated for the entire beam.

Column Axial Deformations : Large axial elongations were measured in the tensile region of the wall, especially in the first story as shown in Fig. 9 (a). Computed axial deformations of the wall boundary column, as expressed as the deformation of outer truss elements, are shown in Fig. 9 (b). Overall deformation amplitudes and hysteresis shapes of the analytical model agree reasonably well with those of the test structure.

DYNAMIC ANALYSIS

In evaluation of possible maximum shear force in the shear wall during an earthquake, multi-degree-of-freedom dynamic (MD) analysis was carried out. The result was compared with that of SDF pseudo-dynamic (SPD) analysis under the same input acceleration, to clarify the effect of higher modes. The NS component of El Centro (1940) record was amplified by 1.5 times and was used in dynamic analysis. The artificial accelerograms in the pseudo-dynamic test runs were not used because the higher frequency components were removed. Retardation time was assumed to be 0.0043 sec. which corresponded to 3 % of stiffness-proportional damping with respect to the fundametal period of the first mode.

Response waveforms in MD analysis and SPD analysis are compared (Fig. 10) for roof-level displacement, base overturning moment, base shear force, wall shear force and column shear force. Displacement, base moment and column shear responses in MD analysis (solid lines) were almost identical to those in SPD analysis (broken lines). However, base shear and wall shear responses in MD analysis were significantly different from those in SPD analysis due to the

effect of higher modes. The maximum wall shear force in MD analysis was about 1.6 times larger than that in SPD analysis. The maximum wall shear force in MD analysis was attained under the lateral load distribution different from that assumed in SPD analysis. Figure 11 (a) shows the load distribution at the mximum wall shear in MD analysis.

Static analysis was carried out under three different lateral load distributions shown in Fig. 11 (b). Base moment-roof displacement relations were identical (Fig. 12 (a)) regardless of the load distribution shapes. At the same displacement (i.e. the same base moment), the base shear force was larger when the centroid level of lateral load distribution was lower, whereas the column shear forces were alomst equal regardless of the load distribution shapes (Fig. 12 (b)). The increment of base shear force due to the change of load distribution pattern was found to be carried by the wall in the wall-frame structure.

CONCLUDING REMARKS

A good correlation was reported between the observed and calculated response in the simulation of the full-scale pseudo-dynamic tests. The nonlinear dynamic analysis method for reinforced concrete wall-frame structures could be made reliable to describe the overall structural response and the local behavior.

Multi-degree-of-freedom earthquake response analysis indicated that the maximum base shear force and wall shear force were larger than the values obtained from the equivalent SDF pseudo-dynamic analysis.

ACKNOWLEDGEMENT

The writers wish to express a sincere gratitude to Drs. H. Umemura and M. Watabe, the Joint Technical Coordinating Committee, U.S.-Japan Cooperative Research Program, for providing an opportunity to actively participate in the project. The study was conducted under the general guidance of Professor H. Aoyama, University of Tokyo.

REFERENCES

1. Okamoto, S., et al, "A Progress Report on the Full-Scale Seismic Experiment of a Seven Story Reinforced Concrete Building - Part of the U.S.- Japan Cooperative Program," BRI Research Paper No. 94, Building Research Institute, Ministry of Construction, 1982.

2. Hiraishi, H., "Planer Tests on Reinforced Concrete Shear Wall Assemblies," Report submitted to Joint Technical Coordinating Committee, U.S.-Japan Cooperative Research Program, Building Research Institute, 1981.

3. Nakata, S., et al., "Tests of Reinforced Concrete Beam-Column Assemblages," Report submitted to Joint Technical Coordinating Committee, U.S.-Japan Cooperative Research Program, Building Research Institute and University of Tokyo, 1980.

4. Takeda, T., et al. "Reinforced Concrete Response to Simulated Earthquakes," Journal, ASCE, Vol. 96, No. ST12, 1970, pp. 2557-2573.

5. Architectural Institute of Japan, "AIJ Standard for Structural Calculation of Reinforced Concrete Structures (1982)," AIJ, 1982.

6. Sugano, S., "Experimental Study on Restoring Force Characteristics of Reinforced Concrete Members (in Japanese)," Doctor of Engineering Thesis, University of Tokyo, 1970.

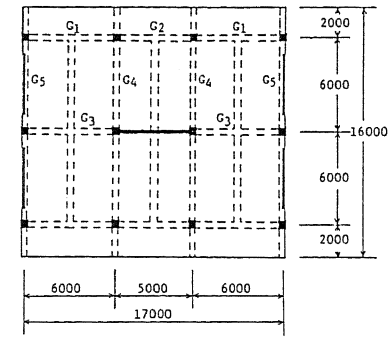

(a) Plan

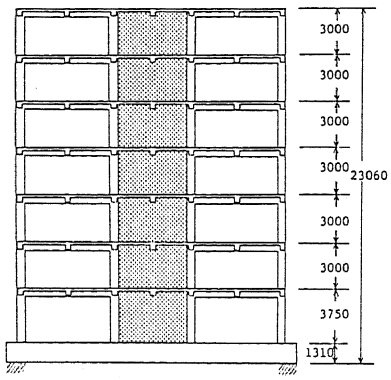

(b) Elevation

Fig. 1 Test Structure

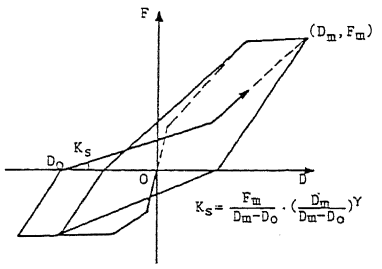

Fig. 4 Takeda-Slip Hysteresis Model

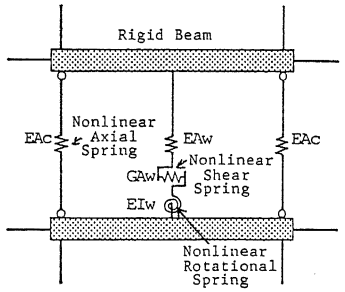

Fig. 2 Wall Model

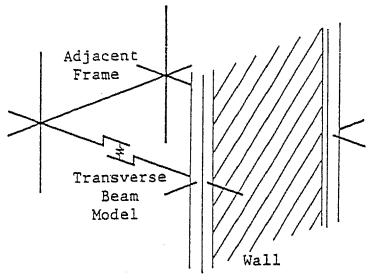

Fig. 3 Transverse Beam Model

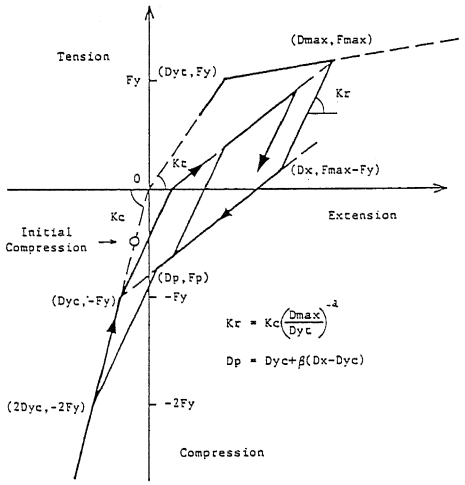

Fig. 5 Axial-Stiffness Hysteresis Model

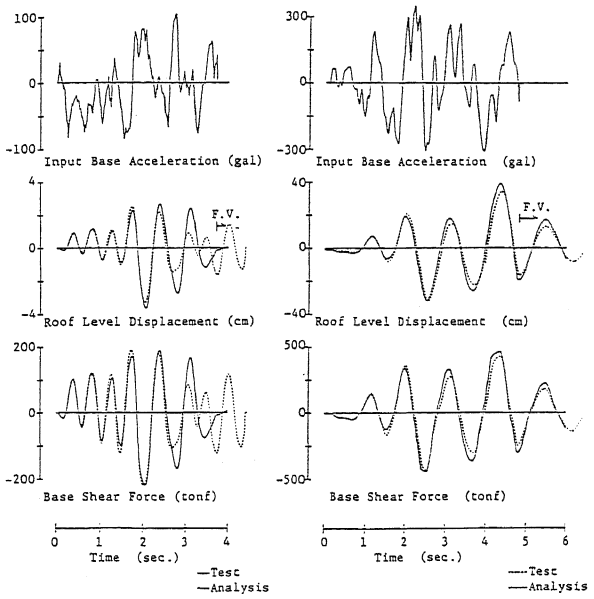

(a) Test SPD-2 (c) Test SPD-4

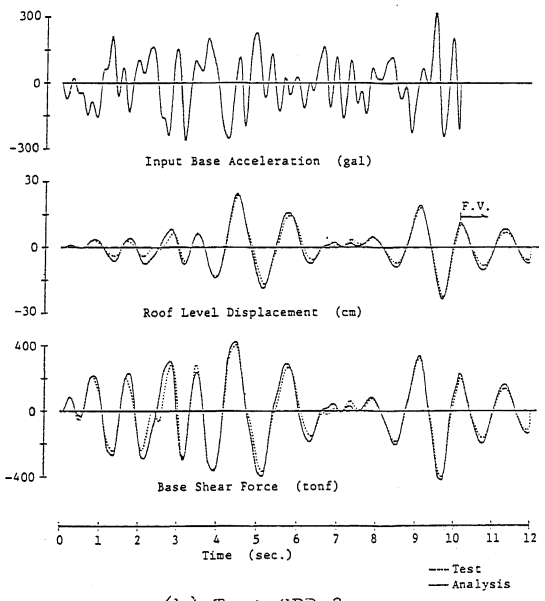

(b) Test SPD-3

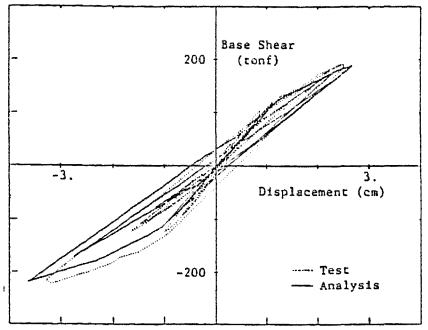

(a) Test SPD-2

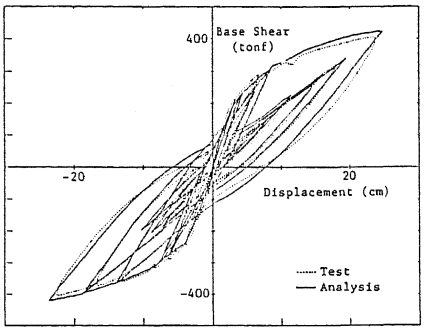

(b) Test SPD-3

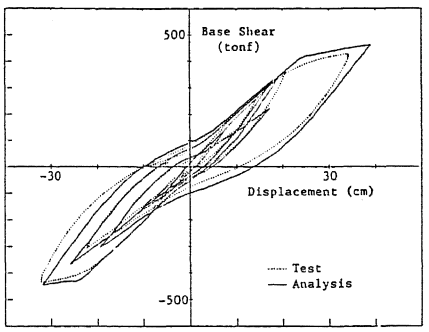

(c) Test SPD-4

Fig. 6 Observed and Calculated Response Waveforms

Fig. 7 Observed and Calculated SDF Hysteresis Relations

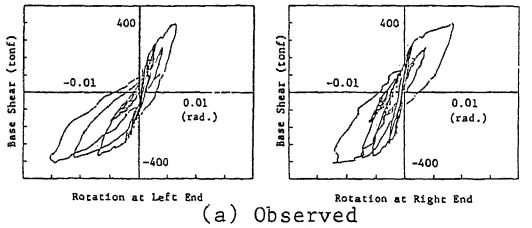

(a) Observed

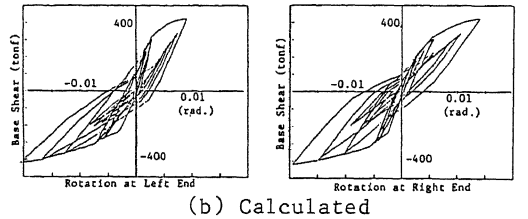

(b) Calculated

Fig. 8 Observed and Calculated Beam End Rotations at Wall Connection [6F]

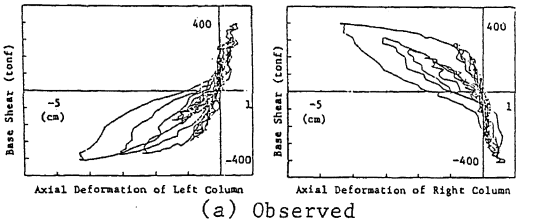

(a) Observed

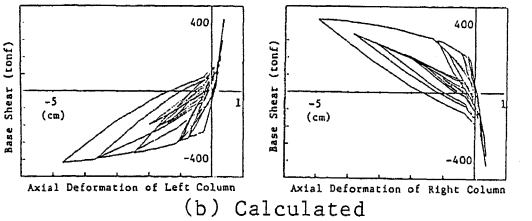

(b) Calculated

Fig. 9 Observed and Calculated Axial Deformations of Wall Boundary Column [1F]

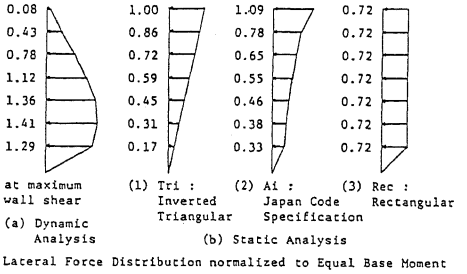

Fig. 11 Lateral Load Distribution

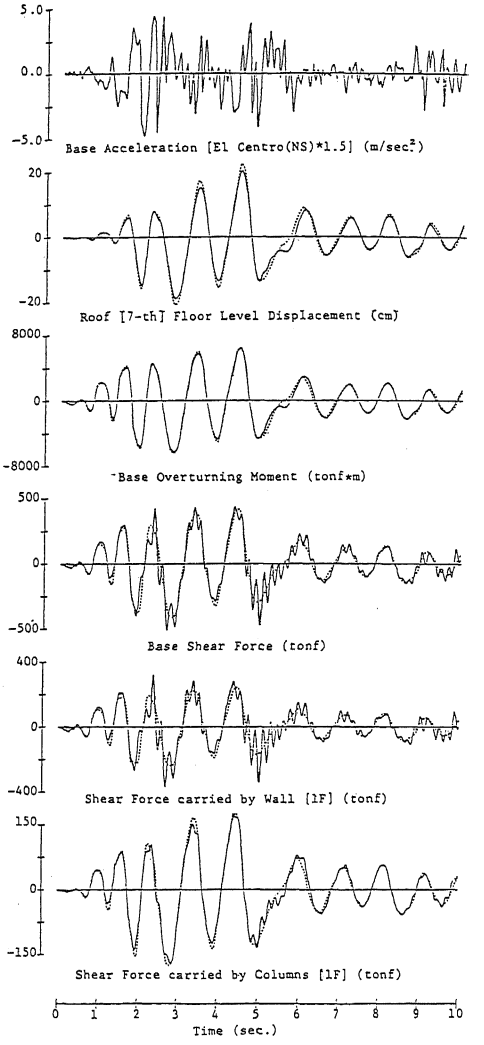

Fig. 10 Response Waveforms in MD Analysis

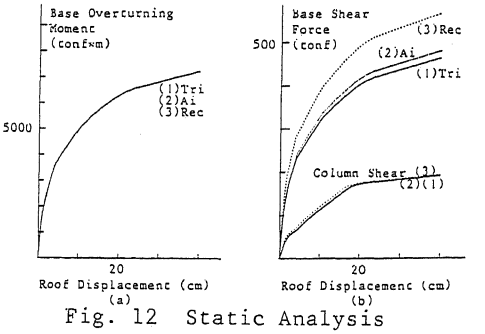

Fig. 12 Static Analysis